Bifurcation structures, dominant modes and the onset of chaotic symbolic synchronization near relative equilibria in the one-dimensional discrete nonlinear Schrodinger equation.

Carlos L. Pando Lambruschini
Instituto de Física , BUAP.

18 de noviembre 2009
IIMAS, UNAM, DF

- ***Dynamics of Sample 3, -0.00625***

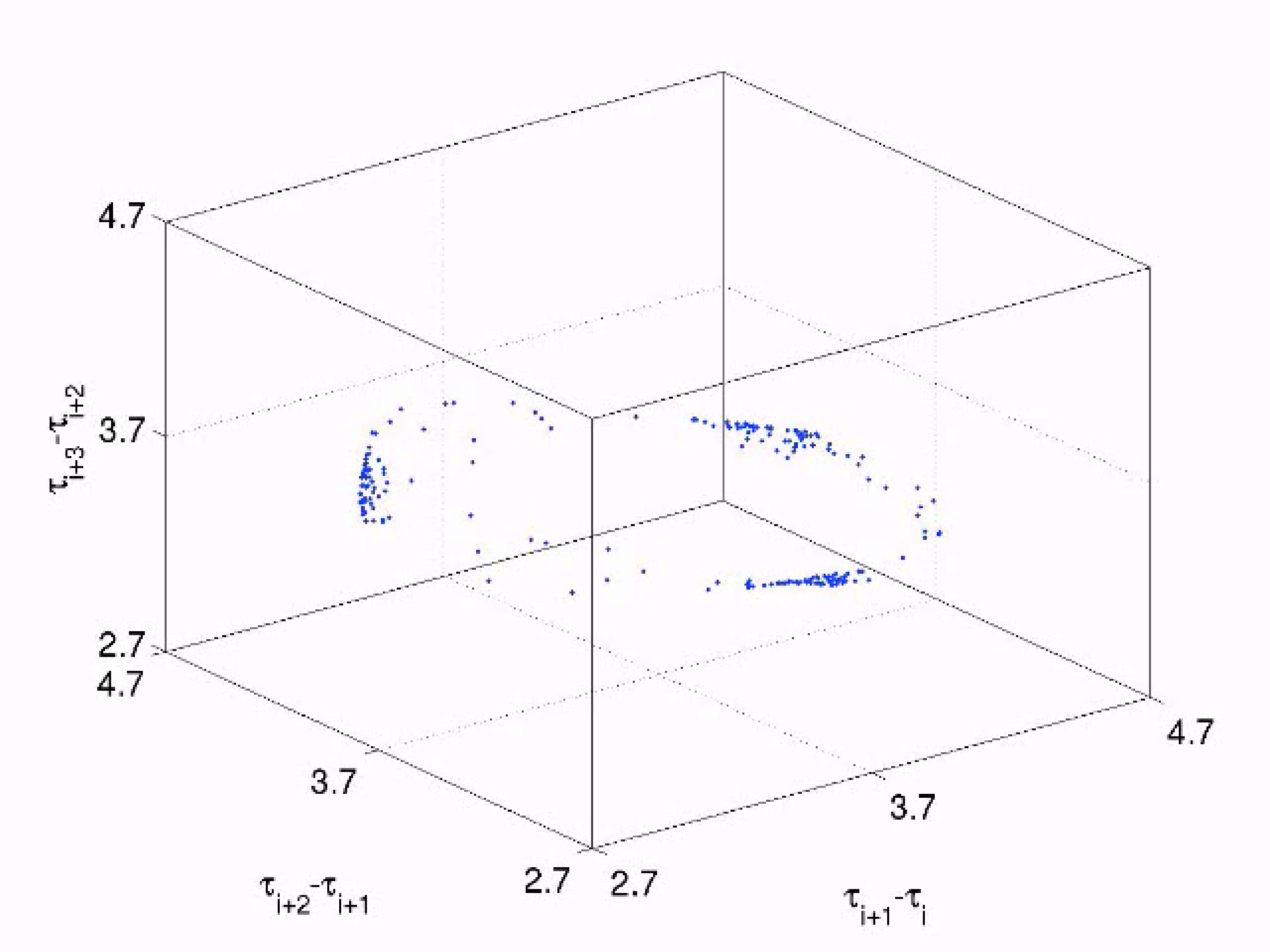

- ***Dynamics of Sample 2, -0.00625***

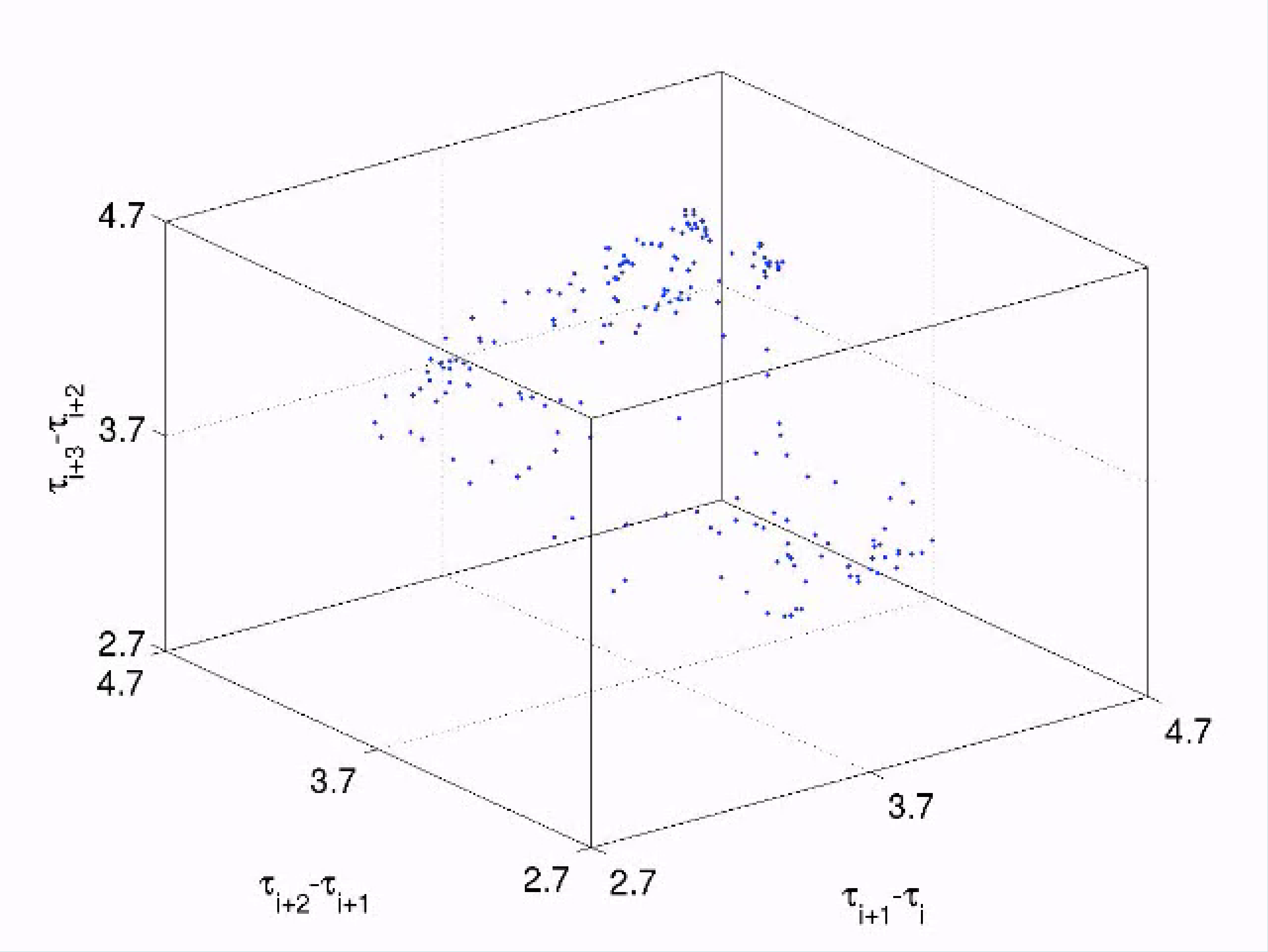

- ***Dynamics Sample 1, -0.00625***

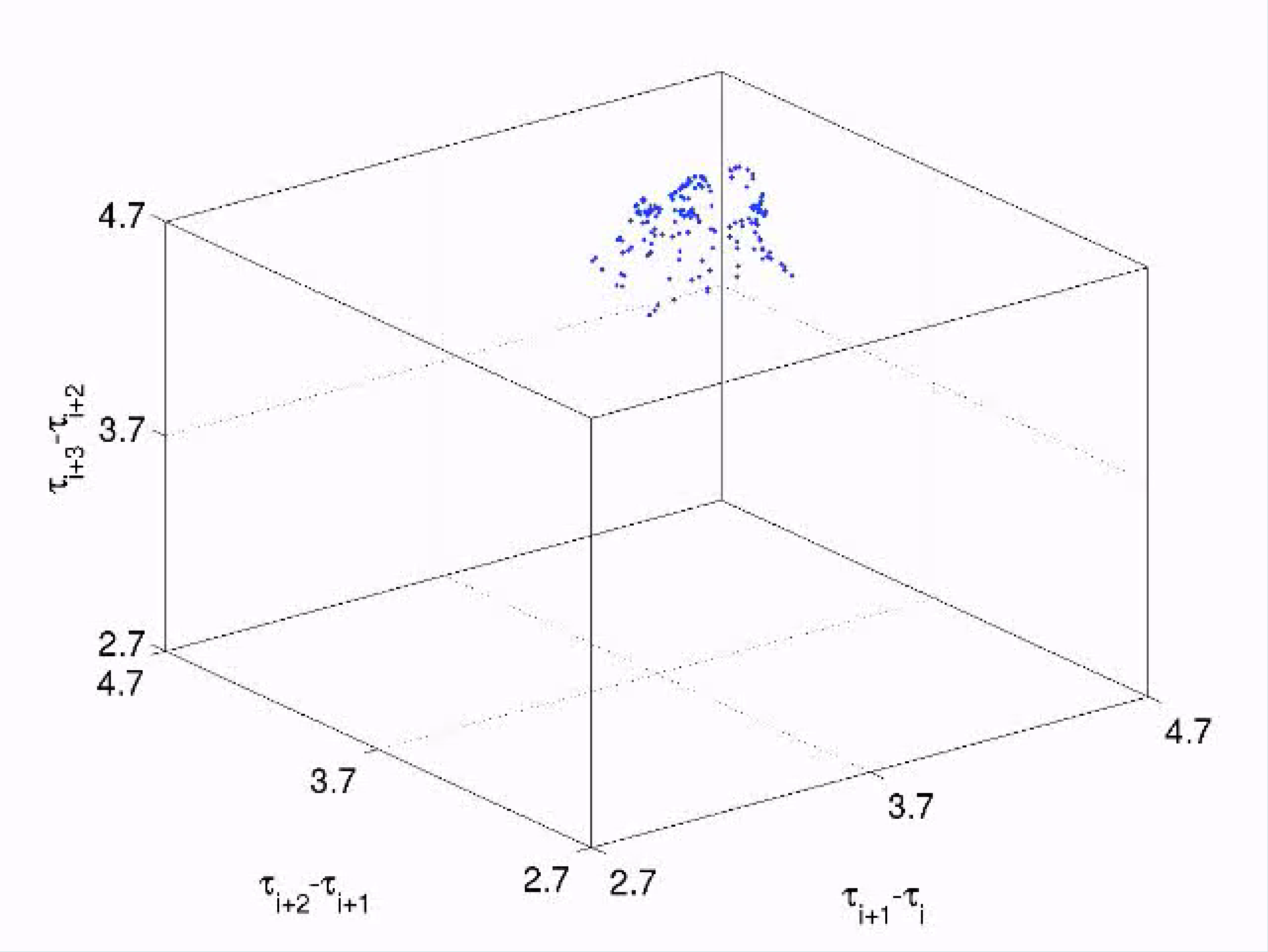

Dynamics for Delta=-0.005, QP

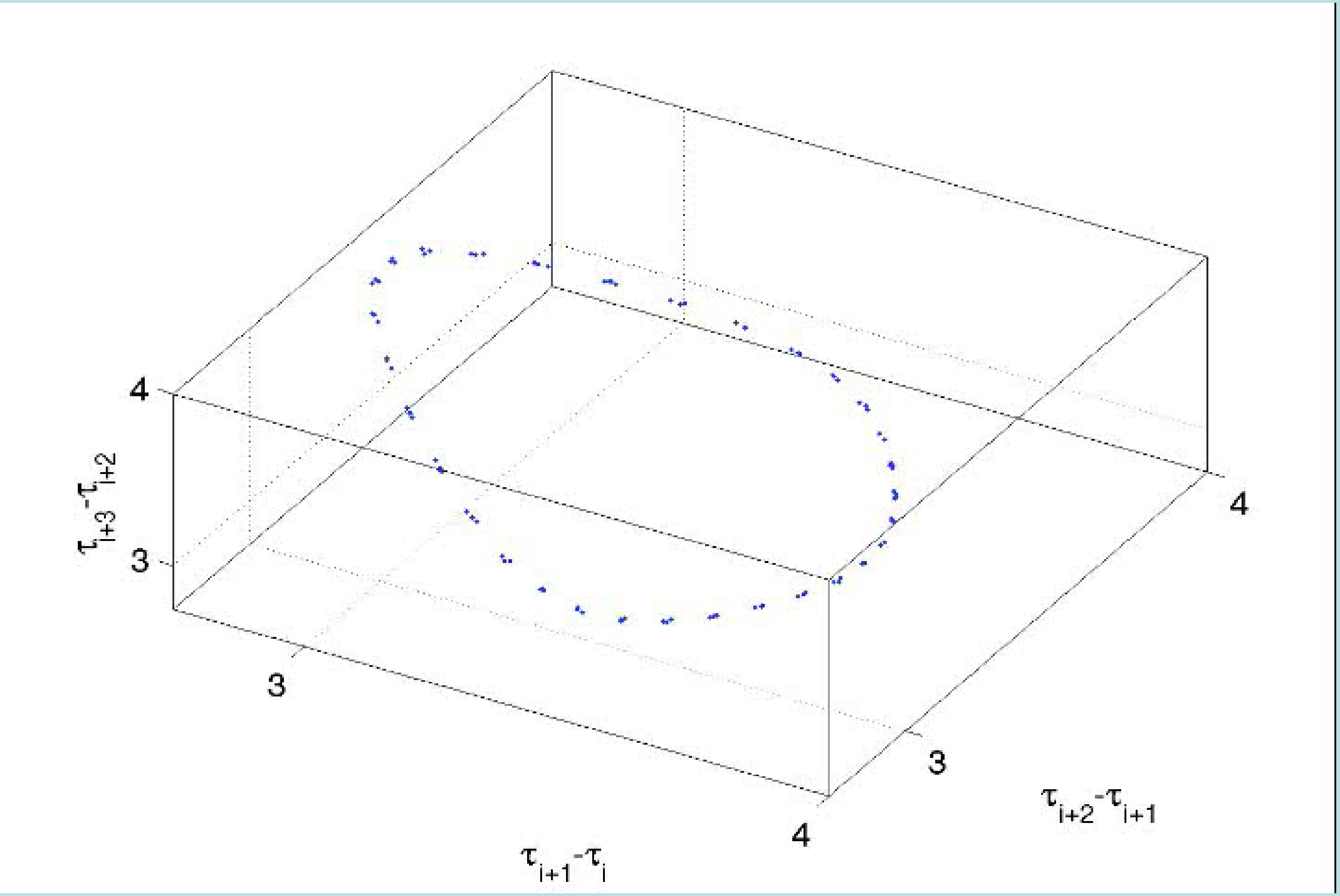

Dynamics for delta=-0.007, global chaos.

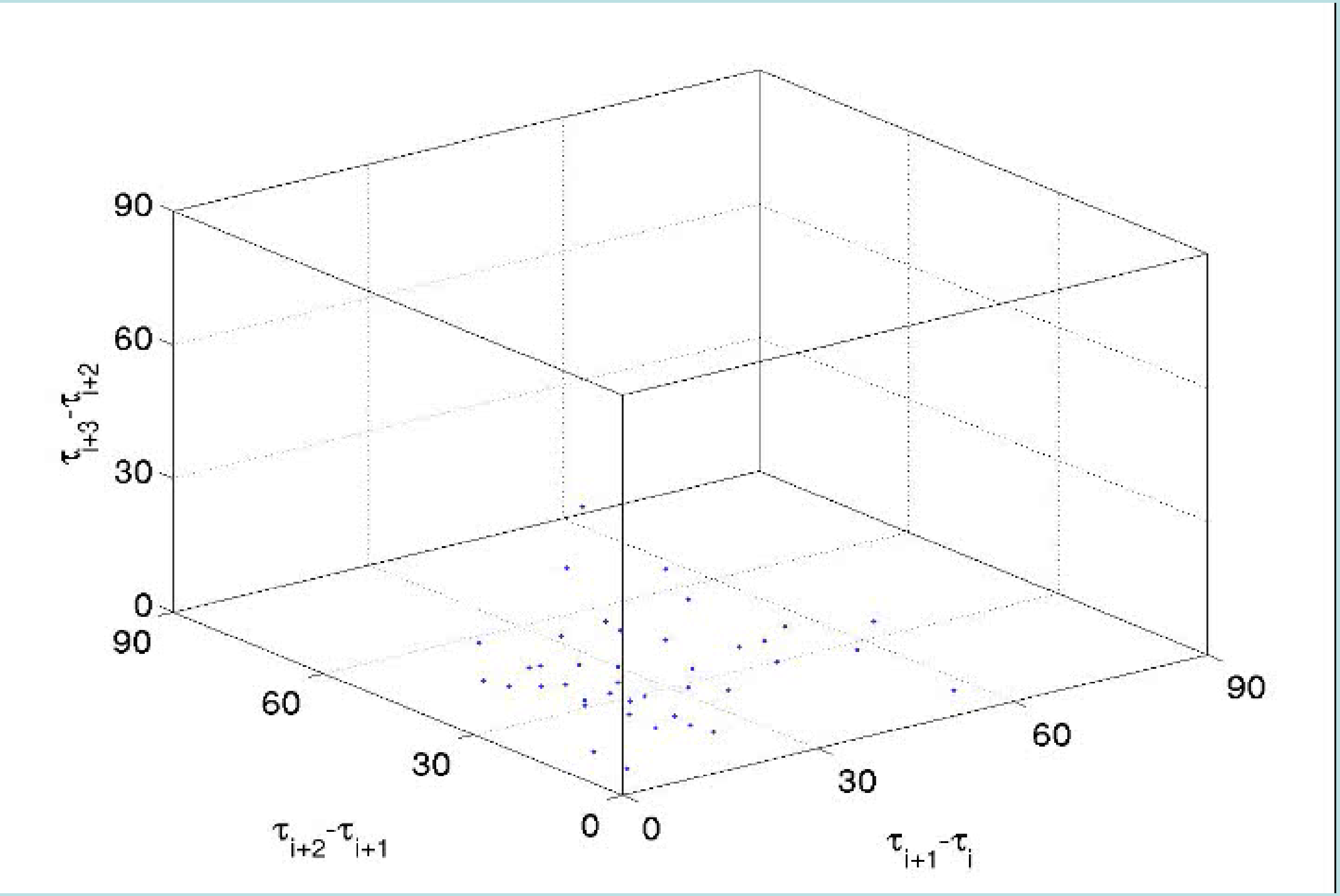

Dynamics for delta=-0.0055.

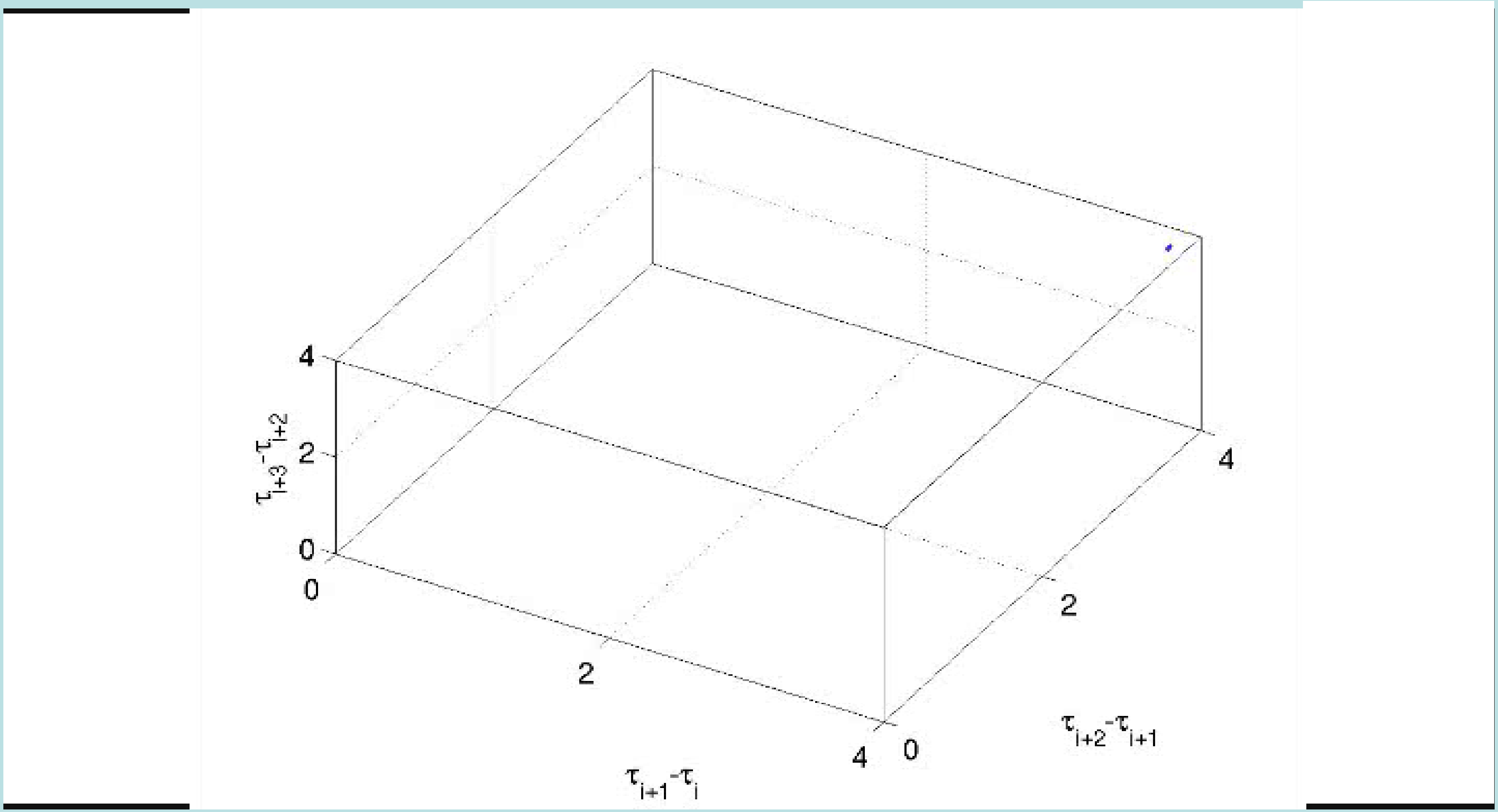

Dynamics for delta=-0.0055, Detail.

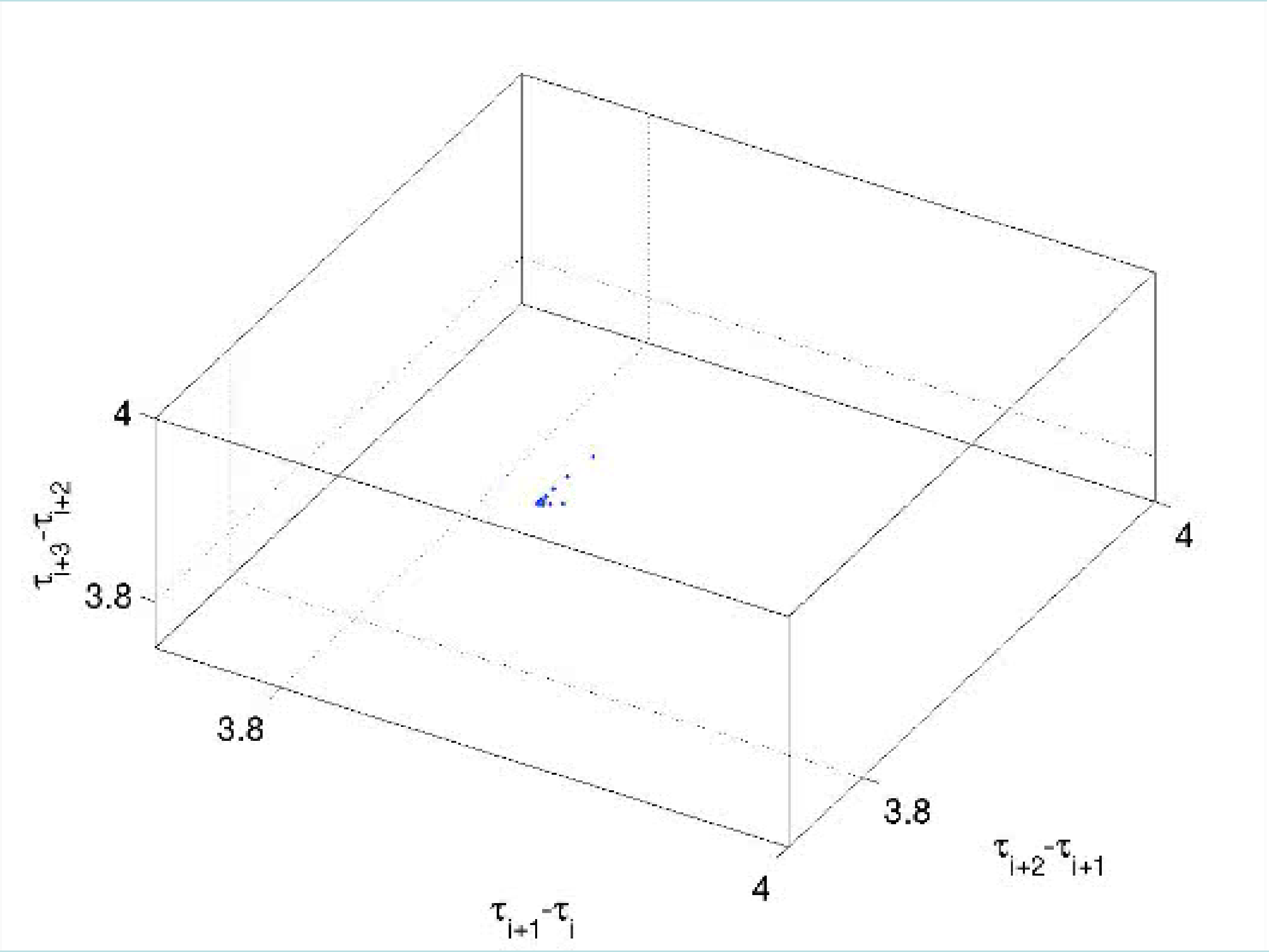

Dynamics for delta=0.0055; geodesic arclenght intervals.

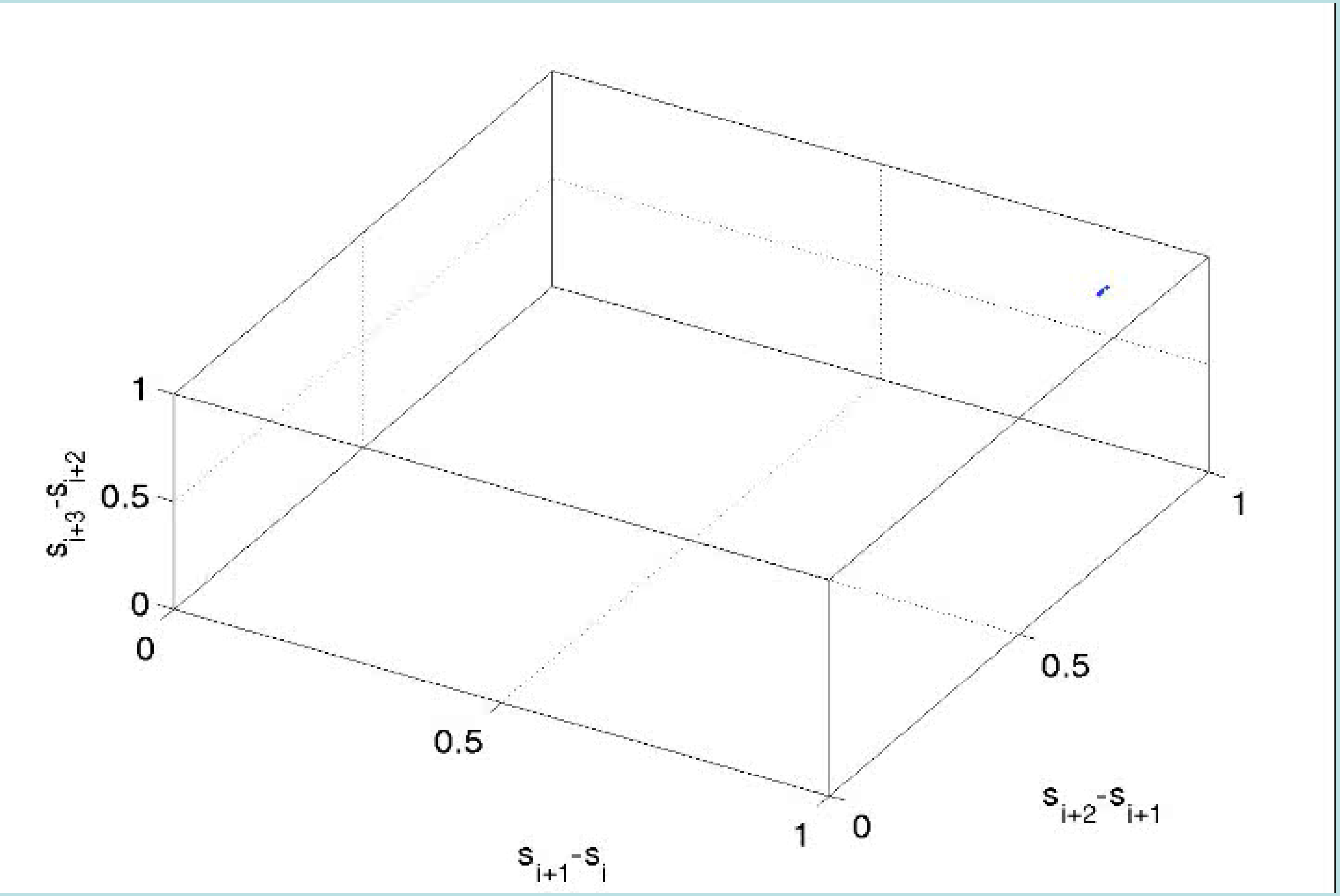

Dynamics for delta=-0.0055; geodesic arclenght intervals. Detail.

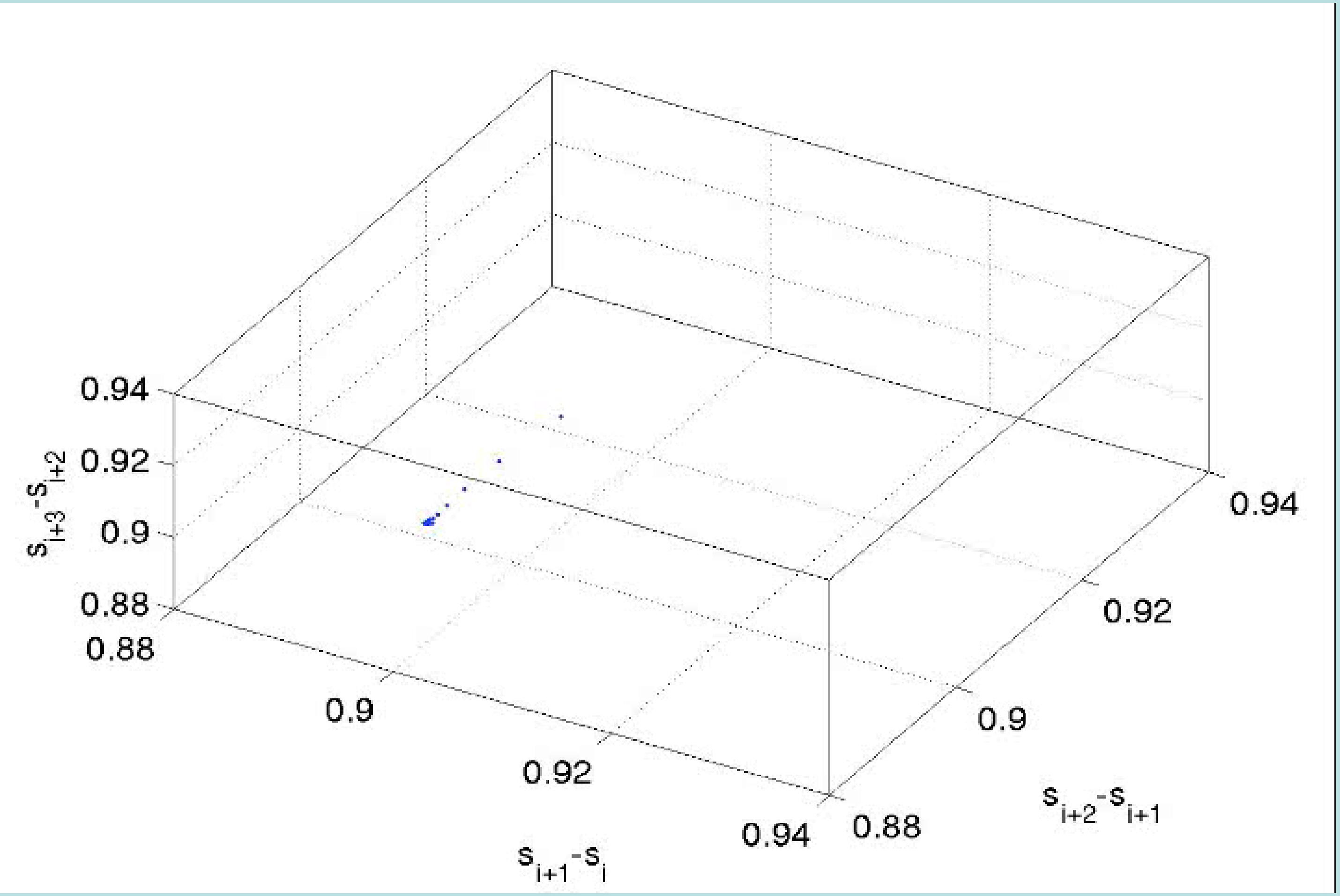

Dynamics for delta=-0.0056, Detail.

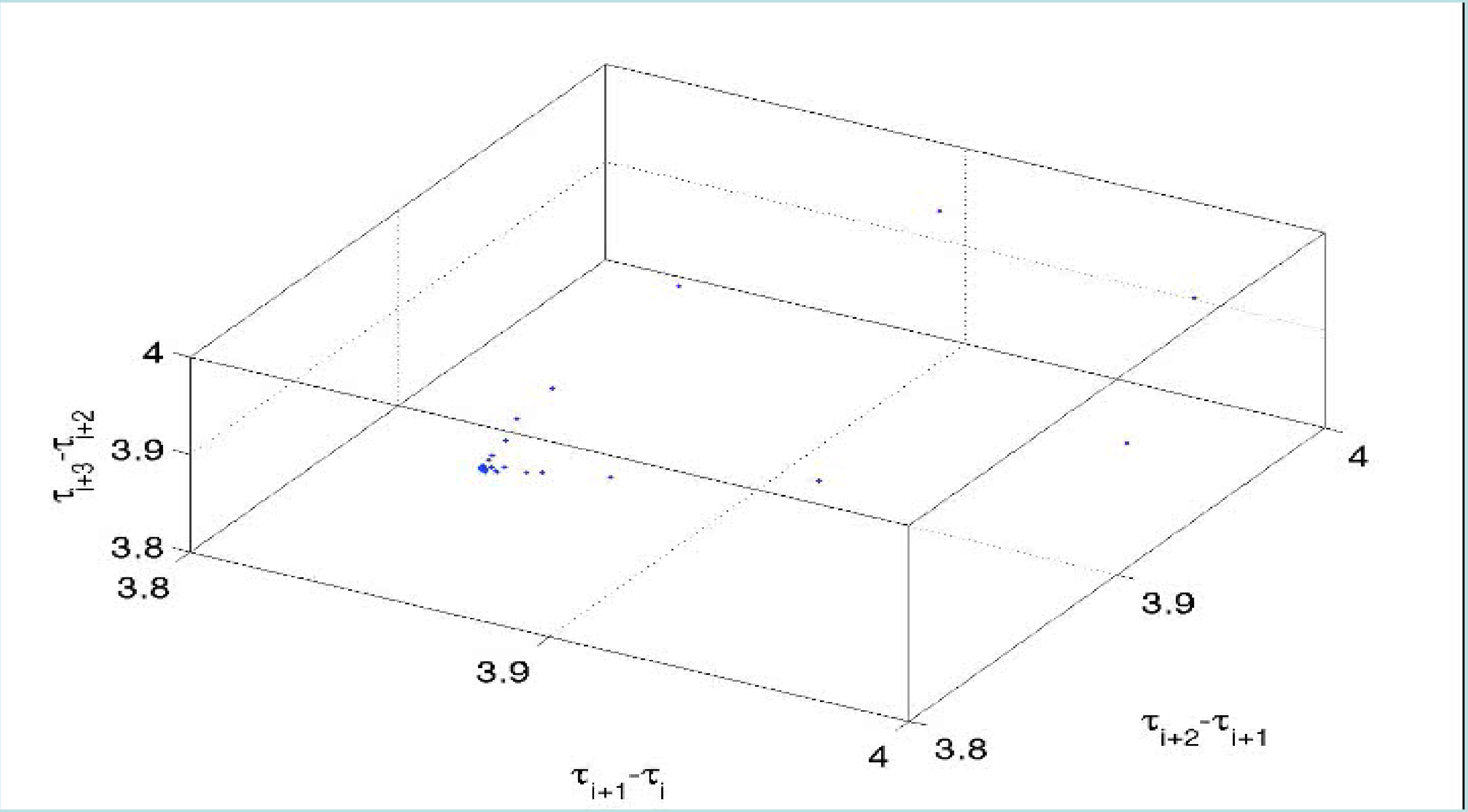

Esquema de la presentación.

(1) What is a BEC (Bose-Einstein Condensate) ?

(2) Basic models (NLSE y DNLSE).

(3) A family of relative equilibria.

(4) The reduced Hamiltonian and its equilibria.

(5) Quasiperiodic dynamics.

(6) Chaotic dynamics.

What is Bose-Einstein condensation (BEC)?

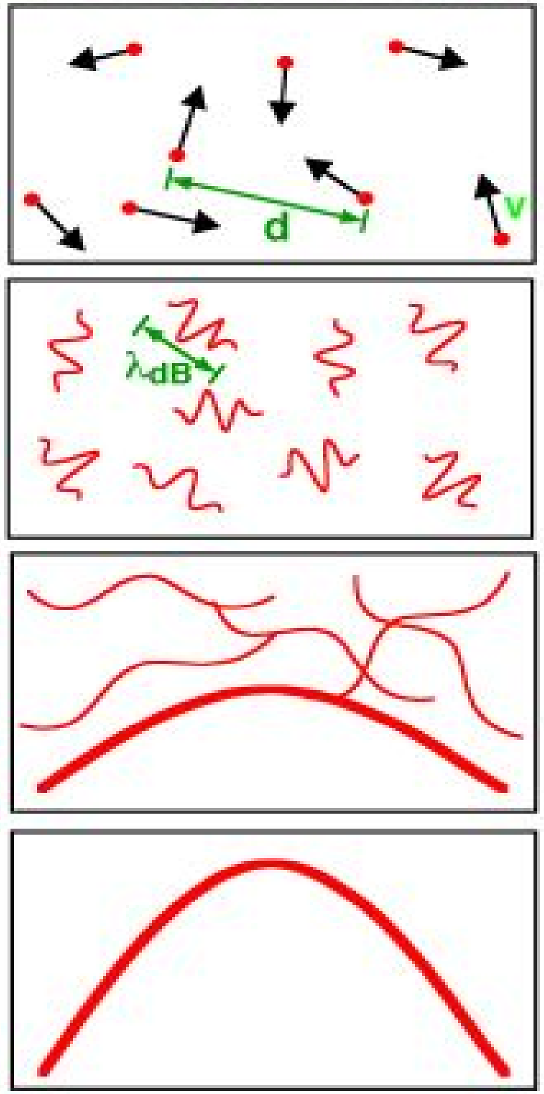

High Temperature T:

thermal velocity v

density d^{-3}

"Billiard balls"

Low Temperature T:

De Broglie wavelength

$\lambda_{dB}=h/mv \propto T^{-1/2}$

"Wave packets"

$T=T_{crit}$: Bose-Einstein Condensation

$\lambda_{dB} \approx d$

"Matter wave overlap"

T=0: Pure Bose condensate

"Giant matter wave"

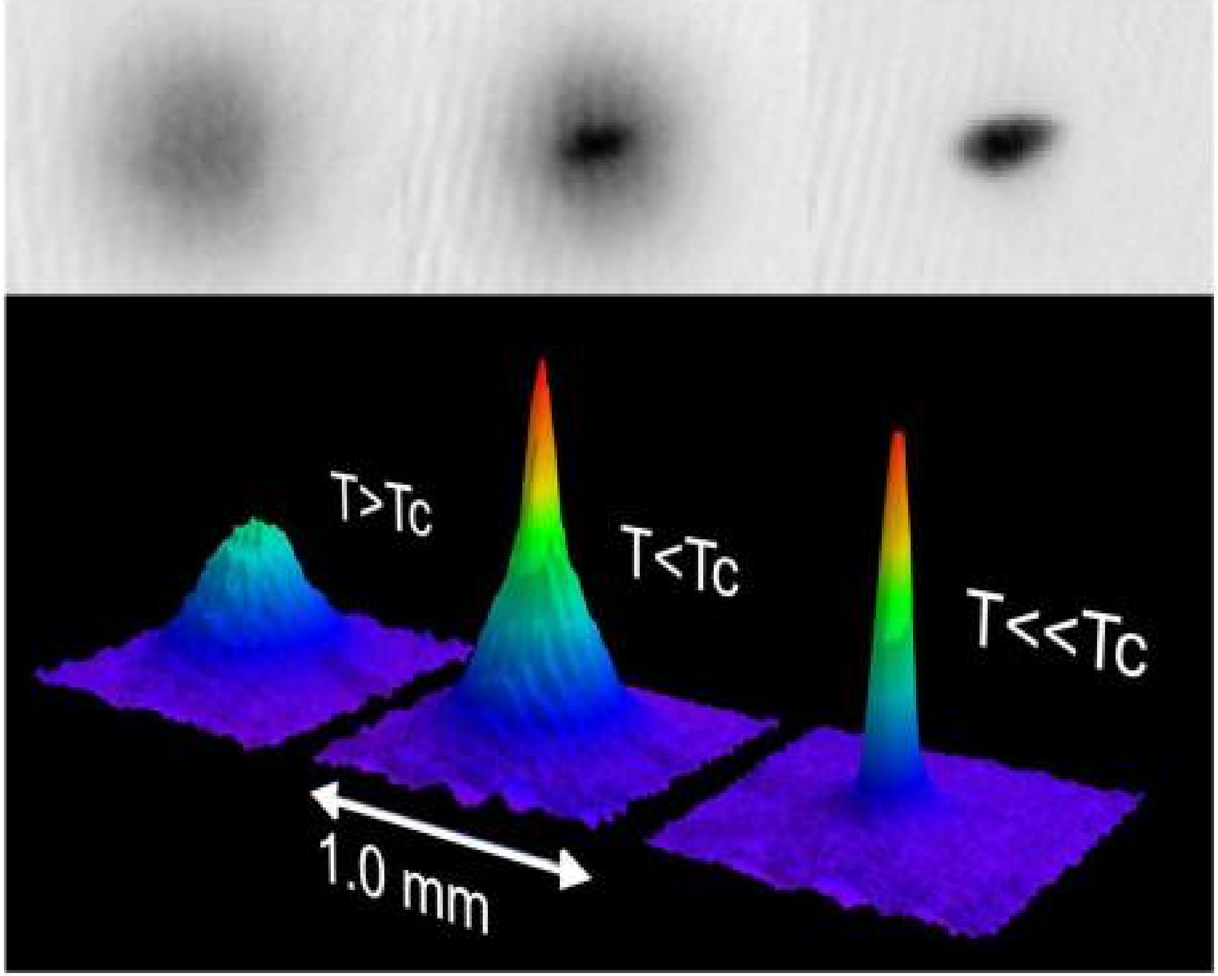

Observation of Bose-Einstein condensation by absorption imaging. Shown is absorption vs. two spatial dimensions.

Basic Models for BEC

At temperature T=0, BEC dynamics is described by the Gross-Pitaevskii equation :

$$\frac{i\partial\Phi}{\partial t} = -\frac{1}{2m}\Delta\Phi + [V + G|\Phi|^2]\Phi$$

The Discrete Nonlinear Schroedinger Equation (DNLSE)

$$i\frac{d\psi_m}{d\tau} + \delta_m\psi_m + (\psi_{m-1} + \psi_{m+1} - 2\psi_m) + 2|\psi_m|^2\psi_m = 0,$$

$$H = \sum_{m=1}^{M} \left(|\psi_m - \psi_{m+1}|^2 - |\psi_m|^4 - \delta_m|\psi_m|^2\right).$$

- Hamiltonian

$$P = \sum_{m=1}^{M} |\psi_m|^2.$$

- Angular Momentum

DNLSE describes many physical systems:

- ***Arrays of optical fibers (1-d).***
- ***Small molecules (Benzene)***
- ***BEC trapped in a multiwell periodic potential (1-d, 2-d)***

Breathers : spatially localized, time periodic (quasiperiodic) and stable solutions of DNLSE, but in infinite one-dimensional lattices.

$$\psi_m = \sqrt{N_m}\exp(-i\theta_m)$$

$$\frac{\mathrm{d}N_m}{\mathrm{d}\tau} = 2\sqrt{N_m N_{m-1}}\sin(\theta_{m-1} - \theta_m) + 2\sqrt{N_m N_{m+1}}\sin(\theta_{m+1} - \theta_m),$$

$$\frac{\mathrm{d}\theta_m}{\mathrm{d}\tau} = 2 - \delta_m - \sqrt{\frac{N_{m-1}}{N_m}}\cos(\theta_{m-1} - \theta_m) - \sqrt{\frac{N_{m+1}}{N_m}}\cos(\theta_{m+1} - \theta_m) - 2N_m.$$

- N_m : action ; θ_m: angle

- **We are considering a ring of seven coupled oscillators.**

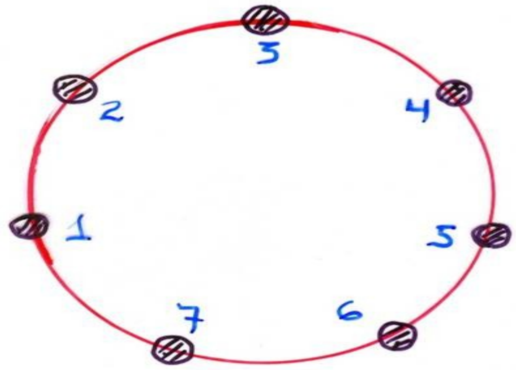

- What happens when a defect is placed at site 3 ?

$H = H_0 + H_1$

$$\begin{aligned}H_0 = {} & 2P - 2\sqrt{N_1N_2} - 2\sqrt{N_2N_3} - 2\sqrt{N_3N_4} - 2\sqrt{N_4N_5} \\ & -2\sqrt{N_5N_6} - 2\sqrt{N_6N_7} - 2\sqrt{N_7N_1} - N_1^2 - N_2^2 - N_3^2 \\ & -N_4^2 - N_5^2 - N_6^2 - N_7^2 - \delta N_3,\end{aligned}$$

$$\begin{aligned}H_1 = {} & 4\sqrt{N_1N_2}\sin^2(\theta_1 - \theta_2) + 4\sqrt{N_2N_3}\sin^2(\theta_2) \\ & +4\sqrt{N_3N_4}\sin^2(\theta_4) + 4\sqrt{N_4N_5}\sin^2(\theta_4 - \theta_5) \\ & +4\sqrt{N_5N_6}\sin^2(\theta_5 - \theta_6) + 4\sqrt{N_6N_7}\sin^2(\theta_6 - \theta_7) \\ & +4\sqrt{N_7N_1}\sin^2(\theta_7 - \theta_1).\end{aligned}$$

The family of relative equilibria that we study is obtained by setting $\frac{dN_m}{d\tau} = 0$, and $\theta_n = \theta_m$, for any $n \neq m$

we can define the frequency of the resulting periodic orbit, *i.e.*, relative equilibrium, by setting $\frac{d\theta_m}{d\tau} = \lambda$, where λ is a constant.

Therefore, these have the form $\psi_m(\tau) = \sqrt{N_m} \exp(-i\lambda\tau + i\theta_0)$.

- ***In particular, we will see that there are Breather-like solutions, along a family with mirror symmetry, which have Liapunov-stability and where the solutions have a few relevant modes.***

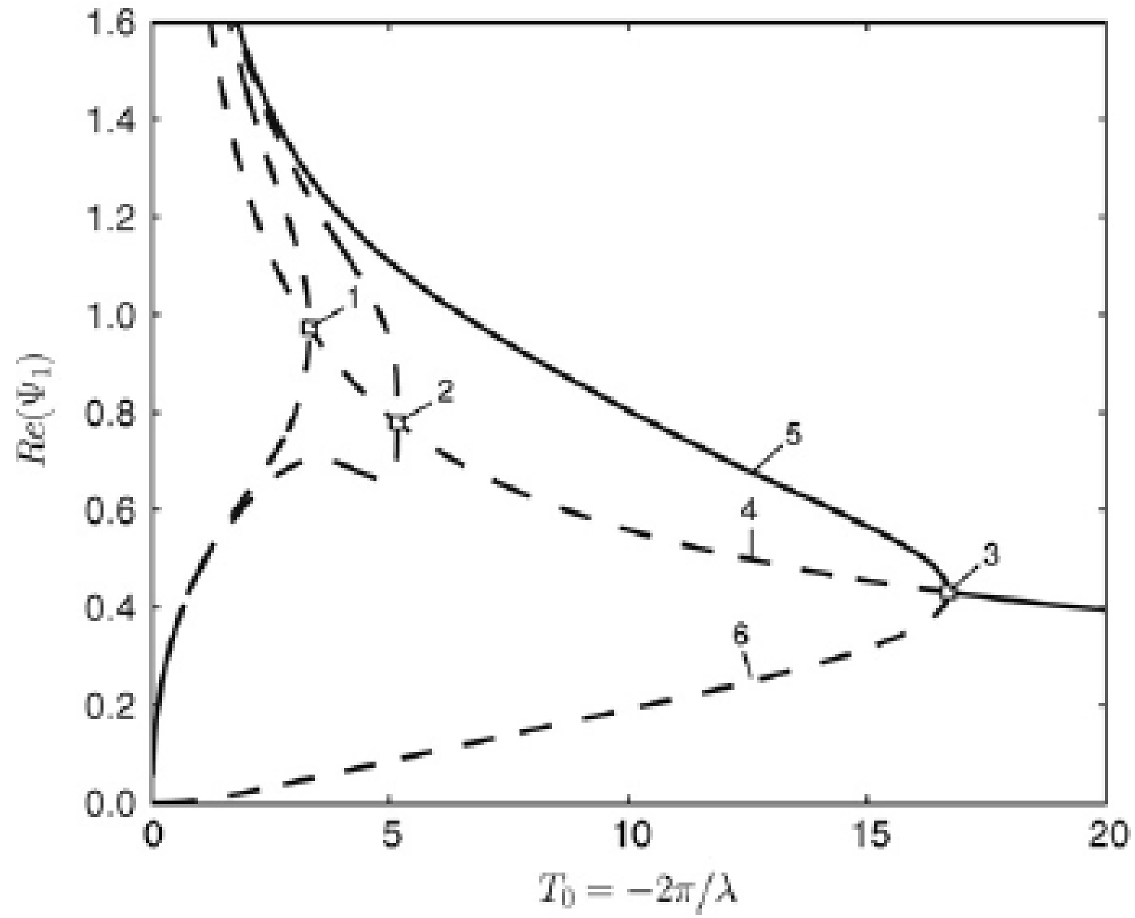

Fig. 1. Plot of $r_1 = \sqrt{N_1} = Re(\psi_1)$ versus the period of the relative equilibrium $T_0 = \frac{-2\pi}{\lambda}$. Here $\delta = 0$. Solid curves denote spectrally stable solutions; dashed curves denote unstable solutions. $Re(\psi_1)$ stands for the real part of ψ_1.

at each of the three bifurcation points along the in-phase family, there are in fact seven families bifurcating, of which only one is shown per bifurcation point. Moreover, as can be seen in Fig. 1, each of the bifurcating families consist of two “legs”.

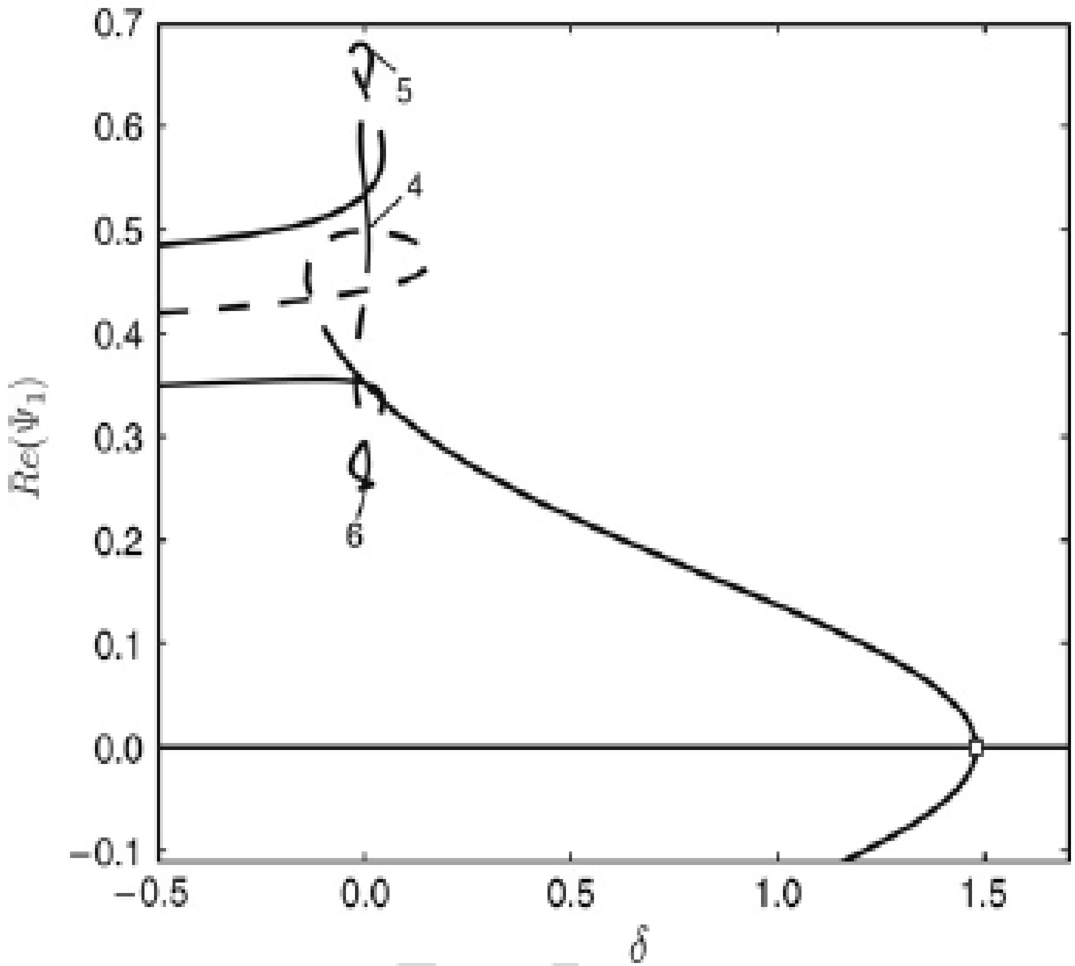

Fig. 2. Plot of the real part of ψ_1, $r_1 = \sqrt{N_1} = Re(\psi_1)$ (see text), versus the defect δ, when $T_0 = 4\pi$.

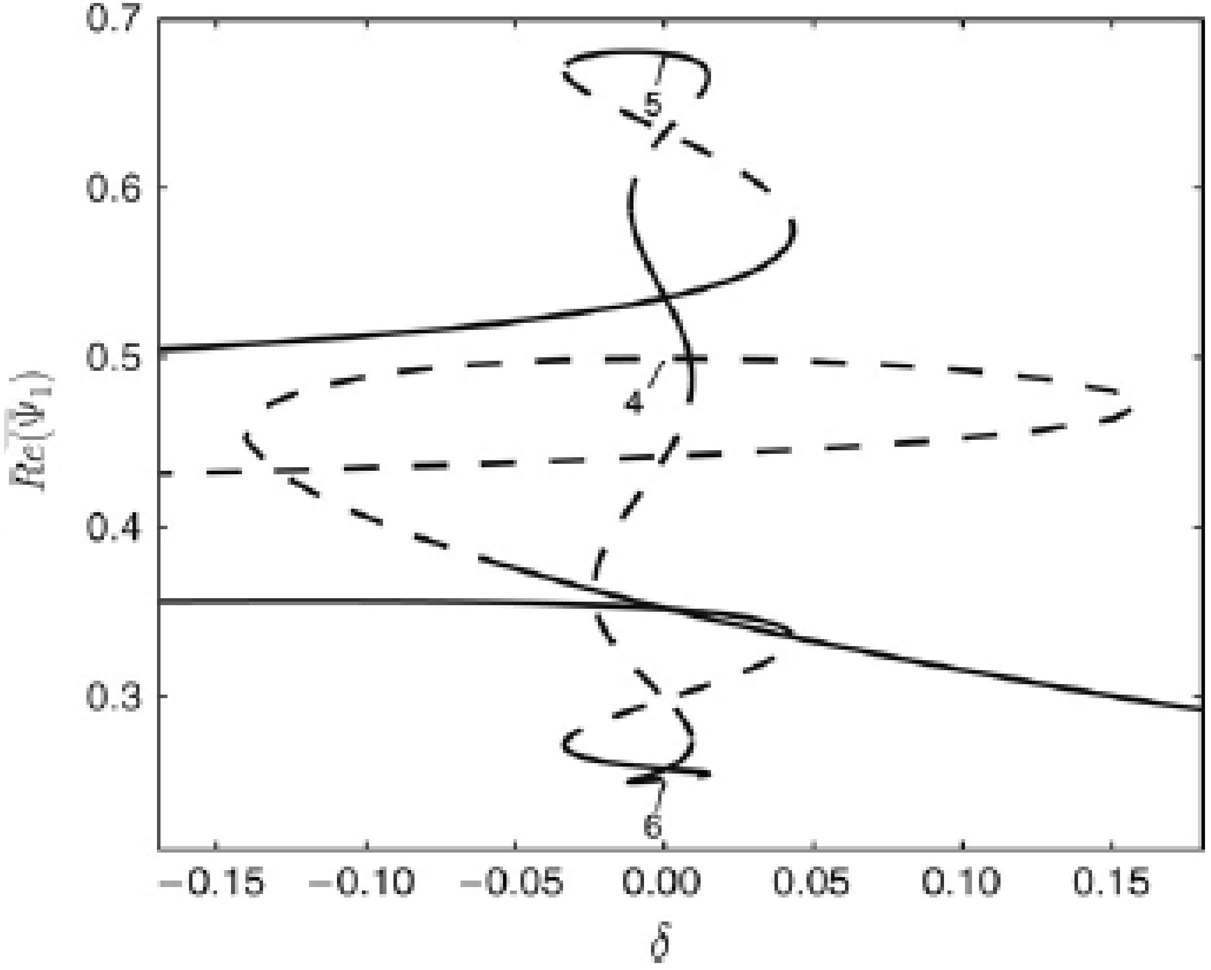

Fig. 3. Plot of the real part of ψ_1, $r_1 = \sqrt{N_1} = Re(\psi_1)$ (see text), versus the defect δ, when $T_0 = 4\pi$. Blow-up of Fig. 2.

In addition to the trivial solution family there appear only two solution branches in Figs. 2 and 3. As one can see, these solution branches contain multiple folds. As a result, one can count 15 solutions at $\delta = 0$, which includes the solutions labeled 4, 5, and 6.

- The reduced Hamiltonian and its equilibria.

A well-defined process, called Hamiltonian reduction, uses the symmetries and the conservation laws to obtain a new family of Hamiltonian systems parametrized by these conserved quantities

when a preserved quantity is in the form of a canonical momentum, its use reduces an N degree-of-freedom system directly to a new $N - 1$ degree-of-freedom Hamiltonian system.

The RH is obtained by making use of the second constant of motion, $P = \Sigma_{i=1}^{7} N_i$, to solve for N_3, where the defect is being located, and by choosing $\theta_3 = 0$.

These conjugate variables are substituted into the Hamiltonian.

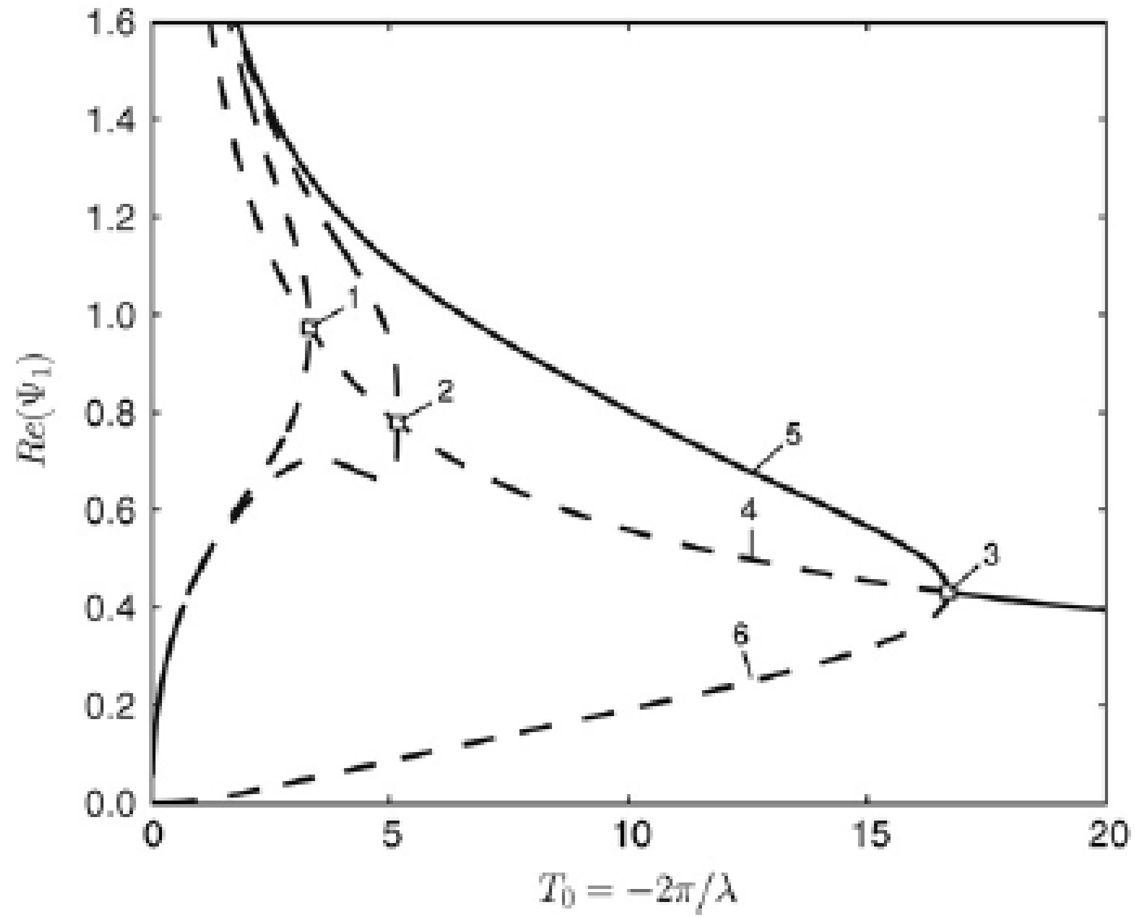

Fig. 1. Plot of $r_1 = \sqrt{N_1} = Re(\psi_1)$ versus the period of the relative equilibrium $T_0 = \frac{-2\pi}{\lambda}$. Here $\delta = 0$. Solid curves denote spectrally stable solutions; dashed curves denote unstable solutions. $Re(\psi_1)$ stands for the real part of ψ_1.

There are six distinct pairs of purely imaginary eigenvalues for the linearized *RH* at Ξ_5 and therefore this is a nonresonant elliptic point for *RH*.

As for the in-phase family and to the right of the bifurcation point 3 in Fig. 1, there are always two equal pairs of purely imaginary eigenvalues, where the number of total pairs is six.

The Hessian of the RH (reduced Hamiltonian) decomposes into two six by six block matrices along the diagonal. The off-diagonal elements are zero.

- ***The Hessian of H_1 is positive definite in theta .***

Convexity of H_0 implies convexity of RH
For the "single-phase solutions".

Convexity of RH implies existence of six
Distinct families of periodic orbits : Nonlinear
Normal modes.
(Liapunov Theorem, Moser-Weinstein).

For point “5”, the conditions of the KAM theorem hold : no-resonance relations And nondegeneracy condition for RH.

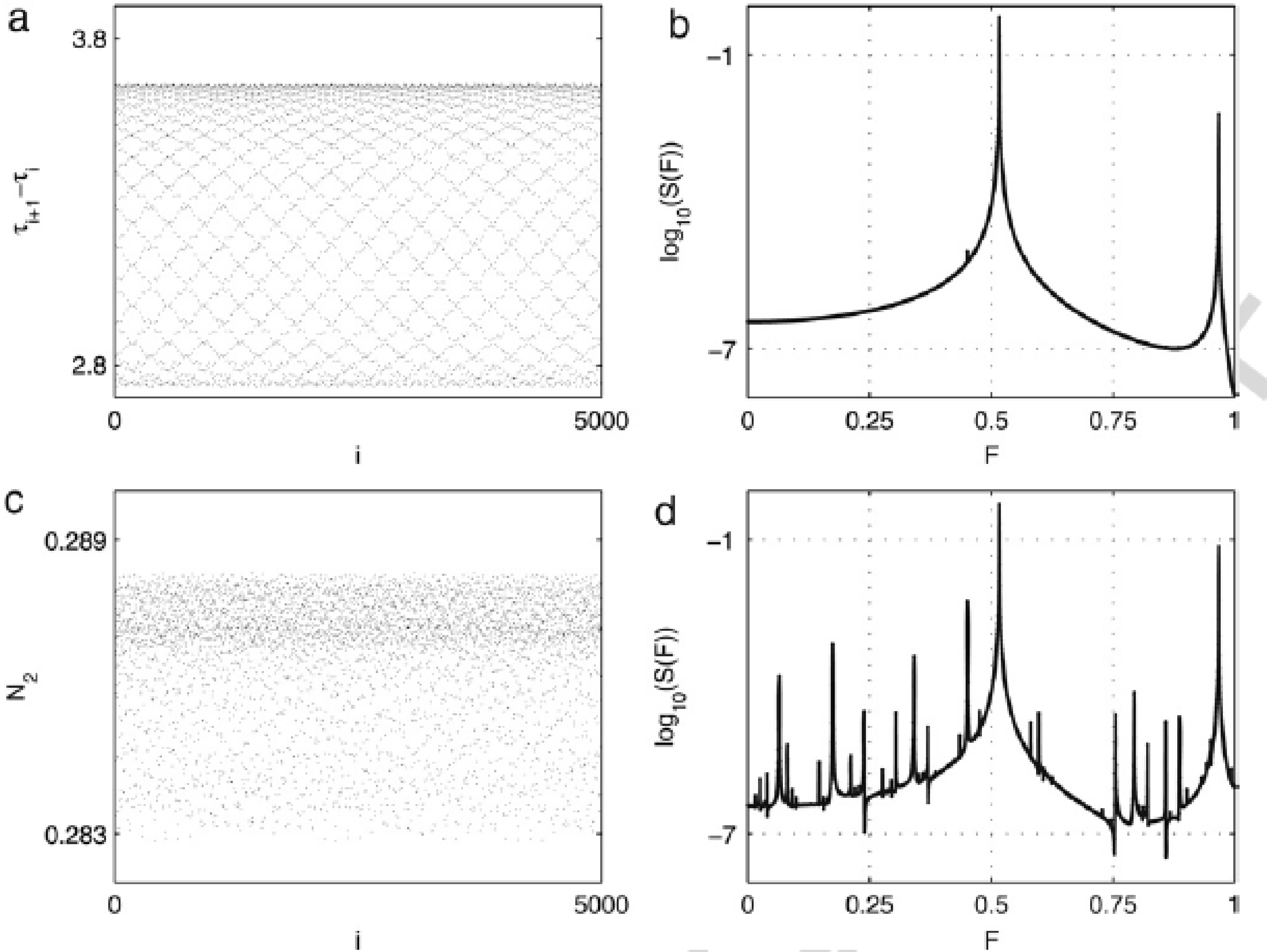
a
3.8
2.8
$\tau_{i+1}-\tau_i$
0
5000
i
b
-1
-7
$\log_{10}(S(F))$
0
0.25
0.5
0.75
1
F
c
0.289
0.283
N_2
0
5000
i
d
-1
-7
$\log_{10}(S(F))$
0
0.25
0.5
0.75
1
F

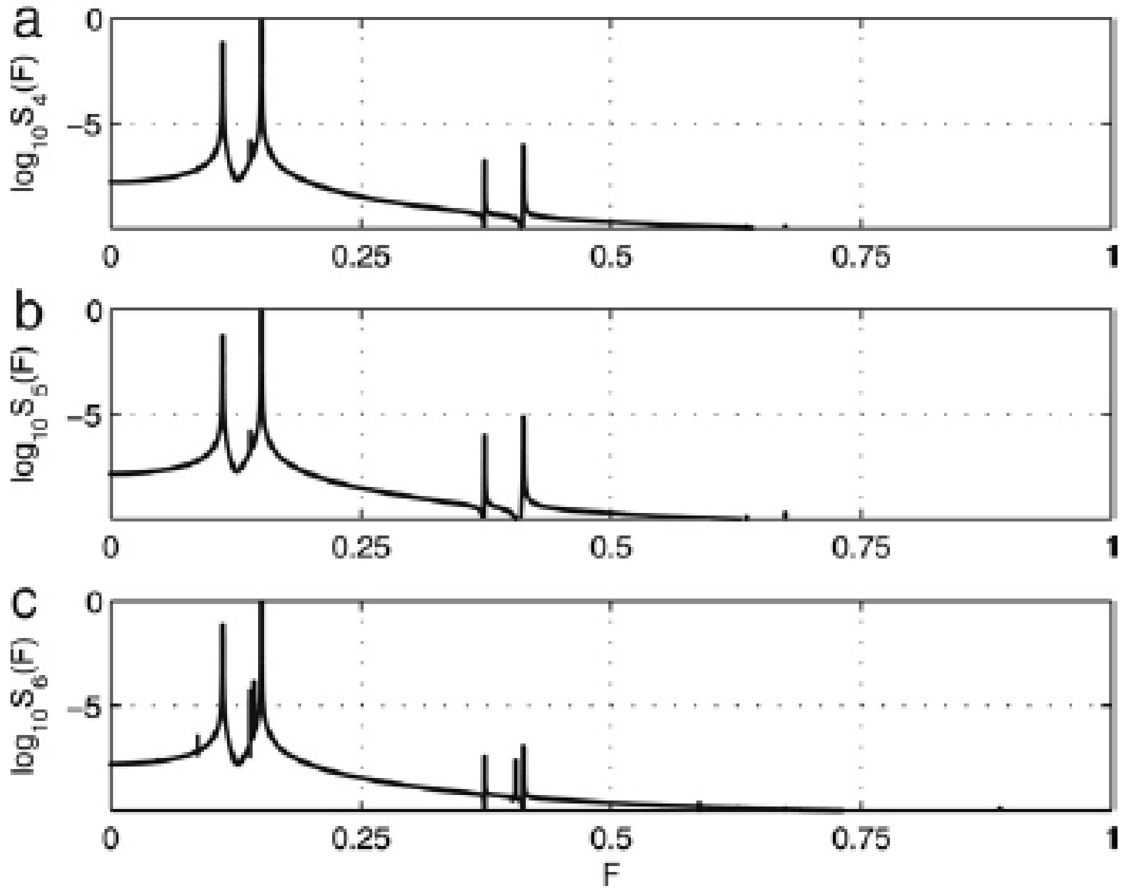

Fig. 9. (a) Power spectral density (PSD), $S_4(F)$, versus frequency F for the continuous time sampling of the slow action $I_4 = \frac{N_2 - N_4}{2}$. (b) The same as (a), but for $I_5 = \frac{N_1 - N_5}{2}$. (c) The same as (a), but for $I_6 = \frac{N_7 - N_6}{2}$. The parameters are the same as those of the previous figures.

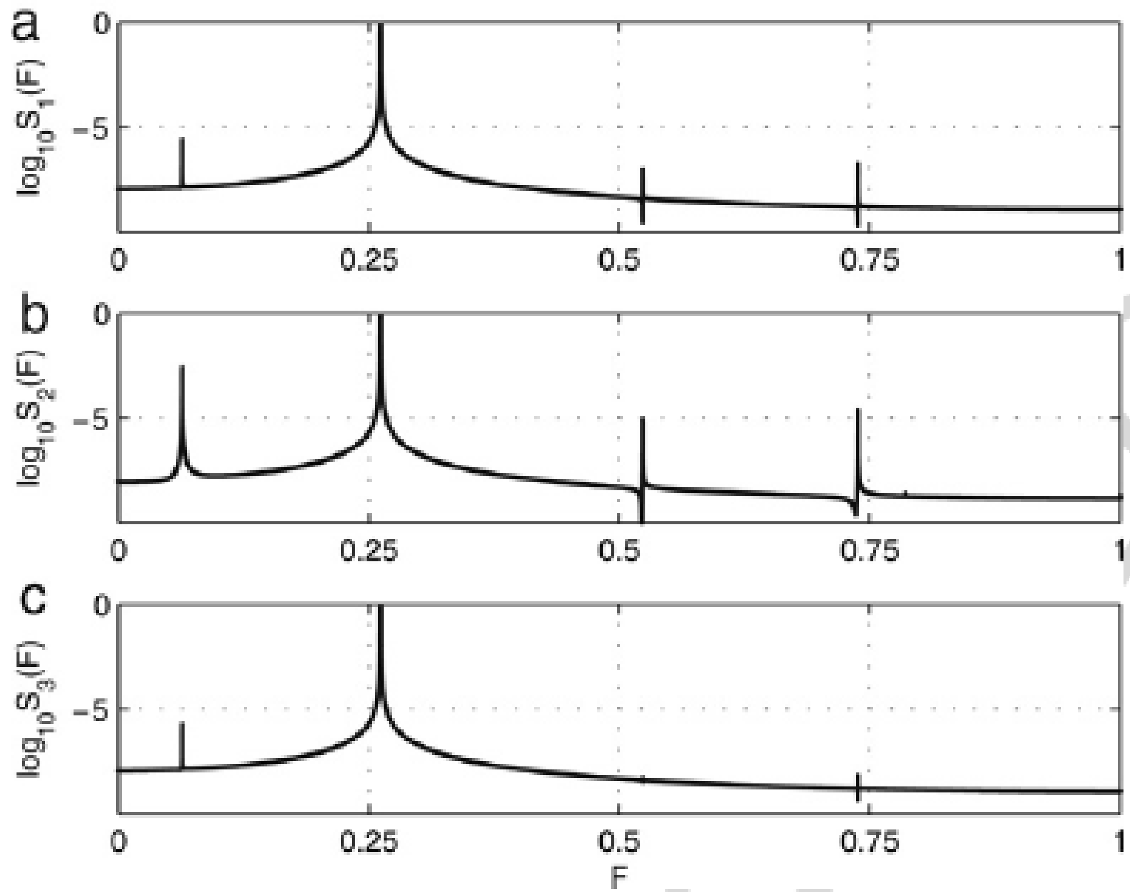

Fig. 10. (a) Power spectral density (PSD), $S_1(F)$, versus frequency F for the continuous time sampling of the fast action $I_1 = \frac{N_2+N_4}{2}$. (b) The same as (a), but for $I_2 = \frac{N_1+N_5}{2}$. (c) The same as (a), but for $I_3 = \frac{N_7+N_6}{2}$. The parameters are the same as those of the previous figures.

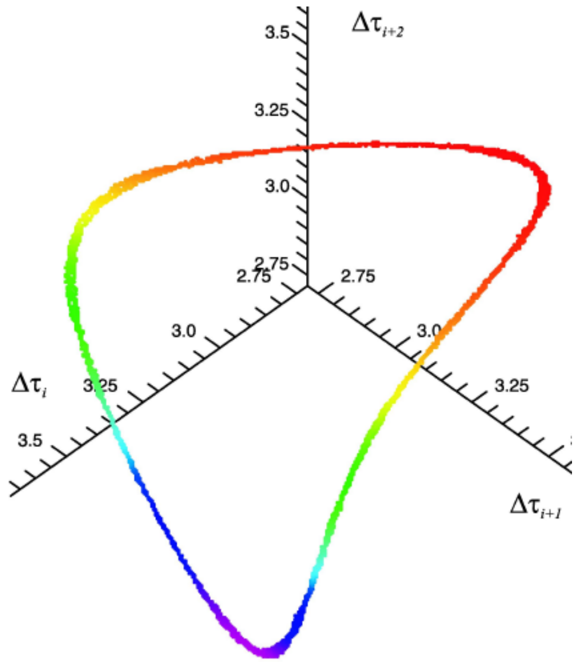

$\Delta\tau_{i+2}$
3.5
3.25
3.0
2.75
2.75
2.75
3.0
3.0
$\Delta\tau_i$
3.25
3.25
3.5
$\Delta\tau_{i+1}$

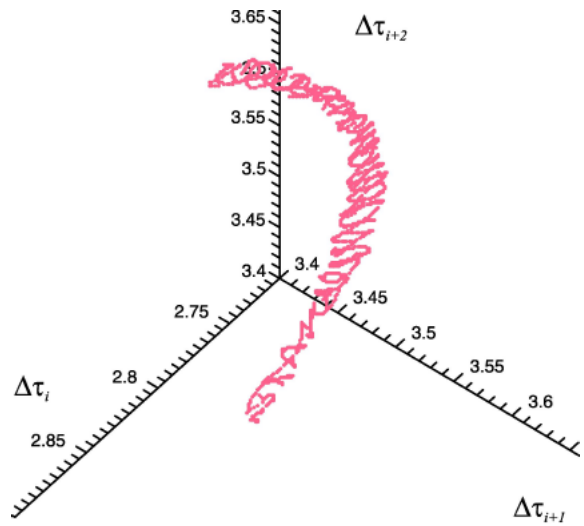
3.65
3.6
3.55
3.5
3.45
3.4
$\Delta\tau_{i+2}$
3.4
3.45
3.5
3.55
3.6
$\Delta\tau_{i+1}$
2.75
2.8
2.85
$\Delta\tau_i$

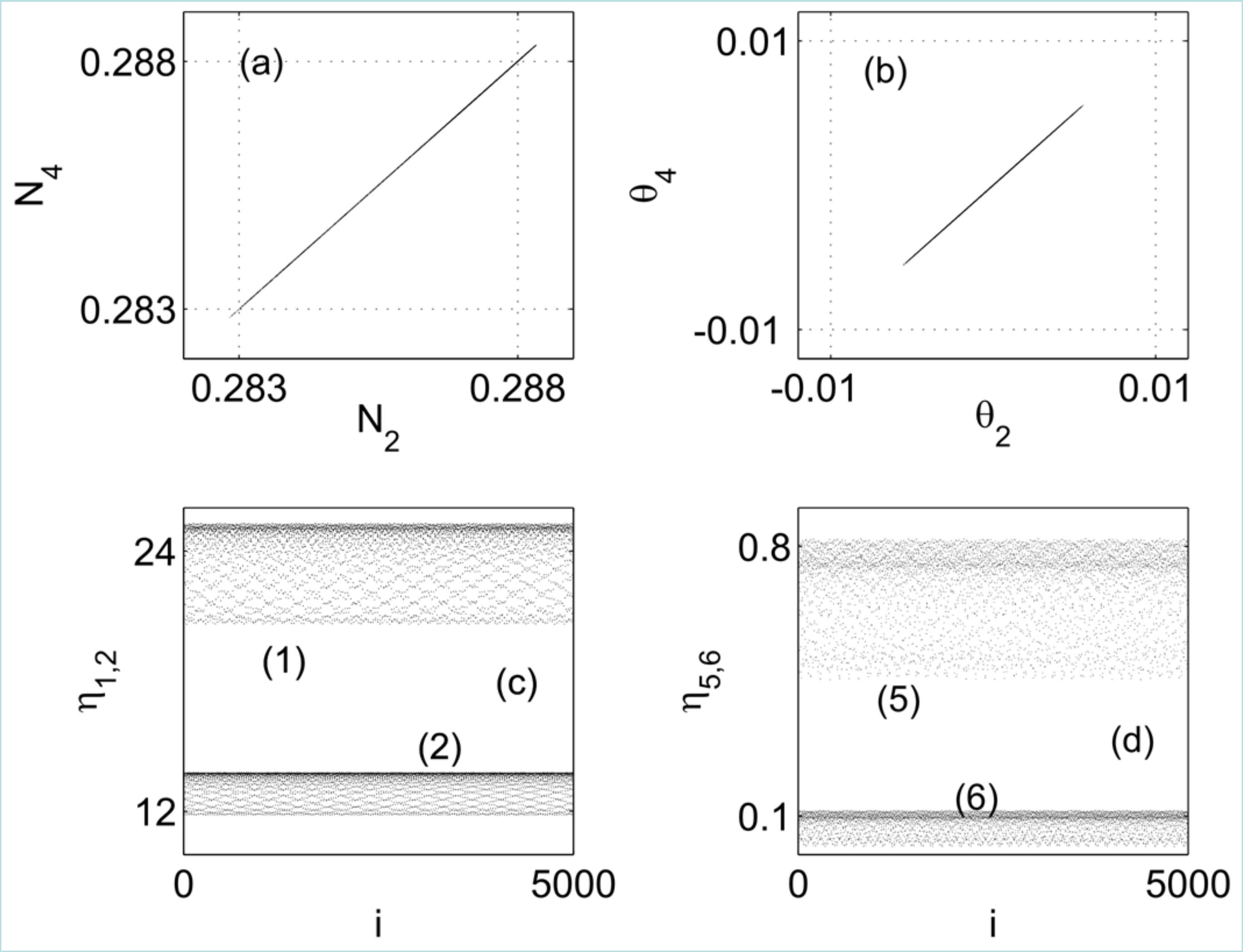
(a)
0.288
0.283
N_4
0.283
0.288
N_2
(b)
0.01
-0.01
θ_4
-0.01
0.01
θ_2
24
12
$\eta_{1,2}$
(1)
(c)
(2)
0
5000
i
0.8
0.1
$\eta_{5,6}$
(5)
(d)
(6)
0
5000
i

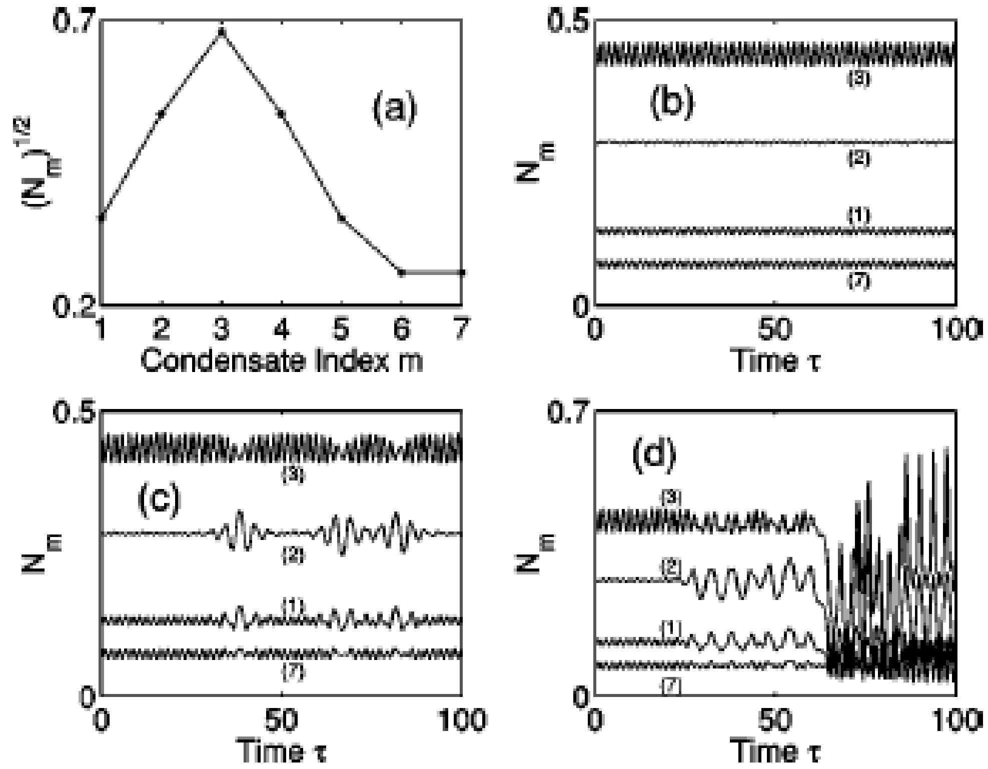

(a) Plot of stationary solution amplitude $\sqrt{N_m}$ versus condensate index m where Γ=2.5. Plot of N_m versus time τ for δ_3 = (b) −0.005, (c) −0.0065, and (d) −0.007. The labels 1, 2, 3, and 7 are the condensate indices. The variable τ has been further rescaled by dividing by 4π.

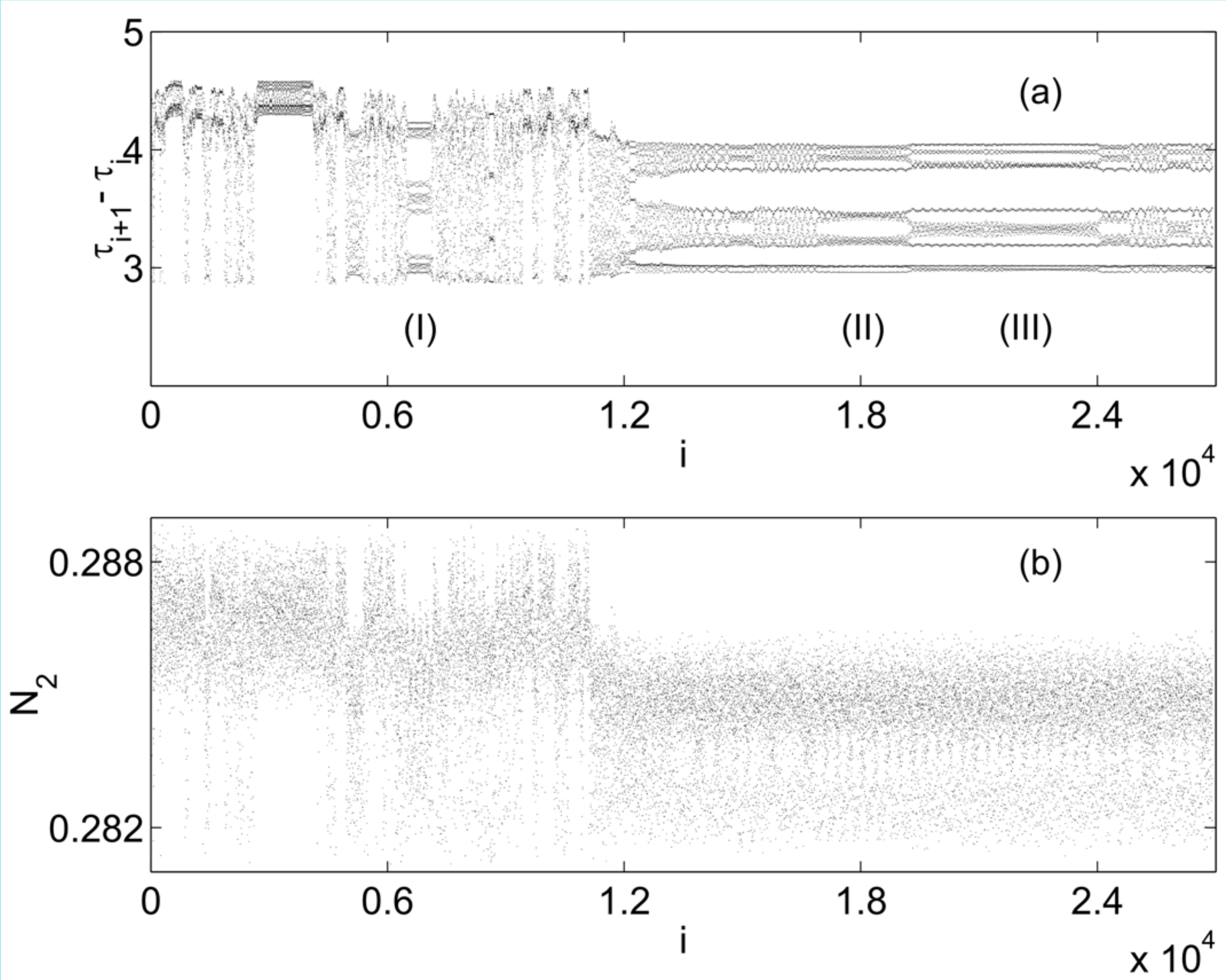

5
(a)
4
3
$\tau_{i+1} - \tau_i$
(I)
(II)
(III)
0
0.6
1.2
1.8
2.4
i
x 10^4
(b)
0.288
0.282
N_2
0
0.6
1.2
1.8
2.4
i
x 10^4

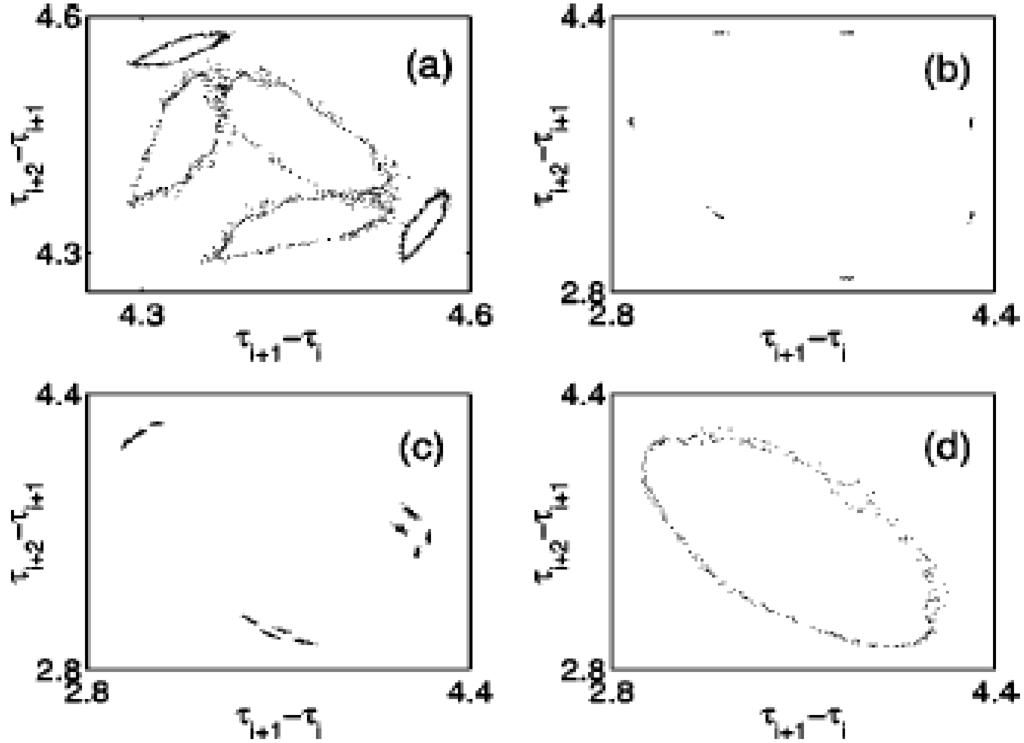

FIG. 4. Return map of the Poincaré cycles, that is, $\tau_{i+2}-\tau_{i+1}$ versus $\tau_{i+1}-\tau_i$ when $\delta_3=-0.0065$ at the Poincaré section for (a) $2700<i<3900$, (b) $8580<i<8670$, (c) $6600<i<7100$, and (d) $5100<i<5380$.

- ***Conclusiones.***

- ***The Hessian of H_0 of a Reduced Hamiltonian H determines the stability in that family of relative equilibria having the "same phase".***

- ***A neighbourhood of stable Breather-like relative equilibria show KAM dynamics and chaotic dynamics (convex and non-convex).***

- ***The time series of the recurrence times is useful in the study of the dynamics of the system, in contrast to following , in the continous time, actions etc.***

- ***¡¡ Mil Gracias por su atención !!***